Journal of Non-Crystalline Solids 358 (2012) 1128–1134

Contents lists available at SciVerse ScienceDirect

Journal of Non-Crystalline Solids

journal homepage: www.elsevier.com/ locate/ jnoncrysol

Glass-ceramics materials from basaltic rocks and some industrial waste

G.A. Khater [a,*], A. Abdel-Motelib [b], A.W. El Manawi [b], M.O. Abu Safiah [c]

[a] National Research Center-Glass Department-Egypt
[b] Faculty of Science, Cairo University, Egypt
[c] Saudi Geological Survey, Saudi Arabia

ARTICLE INFO

Article history:
Received 9 December 2011
Received in revised form 1 February 2012
Available online 27 February 2012

Keywords:
Basaltic rocks;
Ceramic waste;
Crystallization;
Glass-ceramics;
Pyroxenes

ABSTRACT

Preparation of cheap technical glass-ceramic materials by crystallizing glasses derived from Saudi basaltic rocks and ceramic waste materials were investigated. The wastes of ceramic sanitary plants in Saudi Arabia were used. The wastes were formed during the manufacturing of the sanitary ware and used in glass batches, in amounts ranging between 10–50 wt.% of batch constituents. Batches were melted and then caste into discs and rod shapes and subjected to heat-treatment, to induce crystallization. Different techniques were used in the present study including differential thermal analysis, optical and scanning electron microscope, X-ray diffraction indentation, micro hardness, bending strengths, and water absorption. The obtained glass-ceramic materials were mainly composed of pyroxenes, anorthite, olivine and magnetite, of ultra-fine grained and uniform textures as showed by SEM. The obtained glass-ceramic materials are characterized by high values of hardness ranging between 9624 and 10074 MPa, zero water absorption and bending strengths values ranged between 92 and 135 MPa, which makes them suitable for many applications under aggressive mechanical conditions.

© 2012 Elsevier B.V. All rights reserved.

1. Introduction

Glass-ceramics are polycrystalline solids prepared by controlled crystallization of glasses [1]. Controlled crystallization usually involves a two-stage heat-treatment process, namely nucleation stage and crystallization stage [2,3]. Fine-grained, randomly oriented crystals, with some residual glass, without voids, micro-cracks or porosity characterize the glass-ceramic structure [4].

Glass-ceramic materials have a number of outstanding characteristics in composition, which make them favorable for wear and corrosion resistant applications in advanced technology as well as in electronics and medicine. However, due to the high cost of some raw materials (such as $L_{i2}O$, B_2O_3, nucleation agents), and high melting temperatures or special melting conditions, glass-ceramics are relatively expensive materials [5,6]. Basalt, metallurgical slag and fly ash, as bases for glass-ceramics are cheaper than glass-ceramics which are produced from the elementary technical grade oxide powders. Superior abrasion, wear and chemical resistant basalt-based glass-ceramics may be produced from basalt [2].

Senol et al., [7] studied the structural characterization of basalt-based glass-ceramic coatings. These coatings were formed by crystallization at 800,900 and 1000 °C for 1–4 h with the formation of augite, diopside and aluminum diopside phases. The hardness of the coatings varied between 1009 and 1295 H_V depending on crystallization temperature and soaking times.

The use of raw materials, such as igneous or sedimentary rocks, for the production of glass-ceramics materials is of great economic, technological and scientific importance. With proper batch formulation, different types of igneous and sedimentary rocks can be successfully used for the production of crystalline-glass materials of different microstructures and mineralogical constitutions having a wide range of properties. Furthermore, the study of crystallization process taking place in rock melts and their corresponding glasses has a great contribution in petrology field. Minerals capable of wide isomorphous substitutions in their crystal structures, and having the desired properties, may be the bases for production of many valuable crystalline-glass materials [8–13].

Due to the high chemical durability of natural basalts, basalt-like glass-ceramic materials were developed for nuclear waste disposal [14–16] and for vitrification of various hazardous industrial wastes [17–21].

Basalts are the main raw materials for the iron-rich glass and glass-ceramic materials. They are characterized by low viscosity, which allows production of polycrystalline materials by applying short production cycles at low temperature. For these reasons, many researchers continue to study the melting and the crystallization behavior of different igneous rocks, and to characterize the obtained materials [22].

Basaltic rock outcrops are present in great areas in Saudi Arabia, up to 150,000 km^2 and occupy the Western Coast extended and didn't attract yet any attention for industrial application. Most of the exposed basaltic rocks consist of massive to vesicular olivine basalt of Miocene Quaternary age. Saudi basaltic rocks at Harrat Kishb

* Corresponding author. Tel.: 00966505486245; fax: 0096612650597.
E-mail address: Gamal.kh@saudiceramics.com (G.A. Khater).

0022-3093/$ – see front matter © 2012 Elsevier B.V. All rights reserved.
doi:10.1016/j.jnoncrysol.2012.02.010

will be investigated to see if they can be used for the production of cheap glass-ceramic material.

Because glass and glass-ceramics are known to have many commercial applications, the transformation of waste into glass or glass-ceramics provides the opportunity of making useful, marketable products.

Ceramic waste materials used in this investigation are formed as waste materials from Saudi Ceramic plant Saudi Arabia formed during the manufacturing of sanitary ware ceramics. This waste accumulates in large quantities and poses serious problems to the surrounding environment.

The use of waste materials such as ceramic waste, glass cullet, blast-furnace slag and by-pass cement dust for the production of glass-ceramic materials is of great economic technological and scientific importance through proper correction of chemical batch composition.

The aim of this work is to explore the possibility of obtaining a low-cost glass-ceramic material from natural volcanic basaltic rocks of ceramic waste materials. The nature of the phase formation in these materials will be investigated, which will also clarify some typical aspects of the crystallization process and structural characterization in these materials. Saudi basaltic rocks at Harrat Kishb and ceramic wastes formed during the manufacturing of sanitary ware in Saudi Arabia ceramic plants will be used.

2. Experimental procedure

2.1. Batch composition and glass preparation

The collected basalt and ceramic wastes were crushed, milled for 20–30 min in an agate mill, and the obtained powder was sieved under 75 μm. Chemical analysis was performed by XRF. Table 1 shows the chemical analysis of the materials used for batch preparation. Six melted glass compositions were calculated based on basaltic rocks with successive increase in the amount of ceramic waste. These glasses are designated as G0, G10, G20, G30, G40 and G50; where the number indicates the wt.% content of ceramic waste component and the rest is the basaltic rocks (Table 2). The corresponding batches were generally melted in fire clay crucibles at 1400–1450 °C for 2–3 h depending on the composition of the batch mixture. Homogeneous and bubble free glass specimens were obtained. The viscosity of the glass melts was noticed to increase in the direction from G0 to G50. The resulting glasses were stable to uncontrolled devitrification and showed good working properties. After melting and refining the bubble free melt was caste onto a steel plate in the form of discs and rods, and then transferred to a preheated muffle furnace at 550 °C which is then switched off to cool to room temperature.

2.2. Differential Thermal Analysis (DTA)

Differential thermal analysis was carried out using a Shimadzu DTG60 micro differential thermo analyzer, using 60 mg of powdered glass sample, of grain size less than 0.60 mm and greater than 0.2 mm, against Al_2O_3 powder as a reference material. Heating rate of 10 K/min and sensitivity setting of 20 μv/in. were maintained for all DTA runs.

3. Heat-treatment

Choice of the temperature range, for crystallization was guided in most cases by the DTA results. Heat-treatments were also conducted up to 1100 °C at 50 °C intervals with heating rate 10 K/min to follow the transformations of crystallizing pyroxenes phases. Soaking times 3 h were measured from the time at which the sample reached the desired temperature. The choice of this soaking time was due to optimum time, to incite the crystallization process in these glasses.

Glass samples were heated in a muffle furnace from room temperature to the required temperature and kept at the intended temperature for 3 h, after which the furnace was switched off and the samples were allowed to cool inside it to room temperature.

A double-stage heat-treatment schedule was used, to study its effect on the microstructure. Glass samples were first soaked at 720 °C for 1 h and then at 900 °C or 1100 °C for 3 h.

Table 1
Chemical analyses of the raw materials used.

Oxide raw material	SiO_2	Al_2O_3	Fe_2O_3	TiO_2	CaO	MgO	Na_2O	K_2O	L.O.I 1000 °C
Basaltic rock	45.90	16.55	11.80	1.49	10.85	8.30	3.24	0.76	0.41
Ceramic waste	70.14	20.20	0.88	0.60	1.63	0.33	2.45	2.30	1.17

Table 2
Chemical composition of the studied glasses.

Glass no. oxide	G0	G10	G20	G30	G40	G50
SiO_2	45.90	48.32	50.75	53.17	55.60	58.02
Al_2O_3	16.55	16.92	17.28	17.65	18.01	18.38
Fe_2O_3	11.80	10.71	9.62	8.52	7.43	6.34
TiO_2	1.49	1.40	1.31	1.22	1.13	1.05
CaO	10.85	9.93	9.01	8.08	7.16	6.24
MgO	8.30	7.50	6.71	5.91	5.11	4.32
Na_2O	3.24	3.16	3.08	3.00	2.92	2.85
K_2O	0.76	0.91	1.07	1.22	1.38	1.53

Where: G0 = 100% basalt; G10 = 10% ceramic waste + 90% basalt; G20 = 20% ceramic waste + 80% basalt; G30 = 30% ceramic waste + 70% basalt; G40 = 40% ceramic waste + 60% basalt; G50 = 50%ceramic waste + 50% basalt.

3.1. X-ray diffraction analysis

Crystalline phase identification was conducted by X-ray diffraction analysis of the powdered glass-ceramic samples. X-ray diffraction patterns were obtained, using a Bruker D8 Advance, Germany adopting Ni-filtered CuKα radiation. Instrument settings were maintained for all the analyses, using a Si disk as an external standard.

3.2. SEM

The mineralogical constitution and microstructure of almost all the heat treated specimens were examined optically in thin sections using Zeiss scanning electron microscope model XL30, Phillips Holland, the samples etched chemically by 1% HF + 1% HNO_3 solution of 1 s. Then dried and covered by gold film.

3.3. Microhardness measurements

Indentation microhardness of the investigated samples was measured by using Vicker's microhardness indenter (Shimadzu, Type-M, Japan). Testing was made using a load of 100 g. Loading time was fixed for all crystalline samples (15 s). The Vicker's microhardness value was calculated using the following equation: $H_v = A\ (p/d^2)$ kg/mm^2, where A is a constant equal to 1854.5, p is the applied load (g) and d is the average diagonal length (μm). The microhardness values are converted from kg/mm^2 to MPa by multiplying with a constant value 9.8 [23].

3.4. Bending strength and water absorption

Bending strength was evaluated by four point bending strength of the as-prepared glass-ceramics (1000 °C for 3 h), measured on unpolished as-produced test pieces using a universal testing machine (Shimadzu Autograph DCS-R-10TS, Shimadzu) at a crosshead speed of 0.5 mm/min. The reason for using unpolished test pieces is to obtain the strength data from the as-produced samples such as those actually used in building materials and also to avoid chipping of glassy-phase-containing samples by polishing.

Dry the sample in the drier until the weight remains constant, cool in desiccators and weigh (W1) Gms. Place the samples vertically in a metal pot, with no contact between them. Add water so that there is a depth of 5 cm of water until boiling and continue for 2 h. Then maintain water level throughout the test. Stop heating and allow the samples to cool under a stream of water. Remove the sample from the metal pot and remove excess water from each side of a sample with damp cloth and record as (W2) Gms.

$$\text{Percentage of water absorption} = \frac{W2-W1}{W1} \times 100$$

4. Results

Differential thermal analysis of the investigated glasses (Fig. 1) showed various endothermic effects. These small heat absorptions may indicate molecular rearrangement preceding glass crystallization [24]. Exothermic peaks indicating crystallization reaction are also recorded. Limits of crystallization lie around ±30° of the crystallization peaks; because powdered glass, surface nucleation and crystallization tend to obscure the internal structure changes [25].

There are also noticeable gradual increases in the exothermic temperature from G0 to G50. This may be attributed to increase of Al_2O_3 and SiO_2 and to the decrease of Na_2O, TiO_2 and Fe_2O_3 in ceramic waste. The positions of both exothermic and endothermic peaks (Fig. 1) were slightly shifted to higher temperatures for glasses in the order G0 to G40, respectively. In other words the temperatures corresponding to either T_g or pre-crystallization endothermic peaks of the glasses emerged slightly towards higher temperature values as the ceramic waste content ($SiO_2 + Al_2O_3$) was increased in the glass composition.

The broad nature of the exothermic peaks (Fig. 1) indicates the wide temperature range through which crystallization of the investigated glasses may take place. Accordingly glass samples G0–G50 were treated at a temperature in the middle and extreme crystallization range, i.e. 900 and 1100 °C. However, the low peak height indicates the necessity of relatively considerable volume fraction of the crystalline phases. About 3 h at 900 or 1100 °C were found to be the minimum time required to incite the crystallization process in these glasses. This heat treatment process at 900 or 1100 °C for 3 h covers most of the thermal variations appearing on their DTA curves (Fig. 1).

Table 3 summarizes the DTA peak temperatures, thermal effects and corresponding structural changes resulting in the studied glasses.

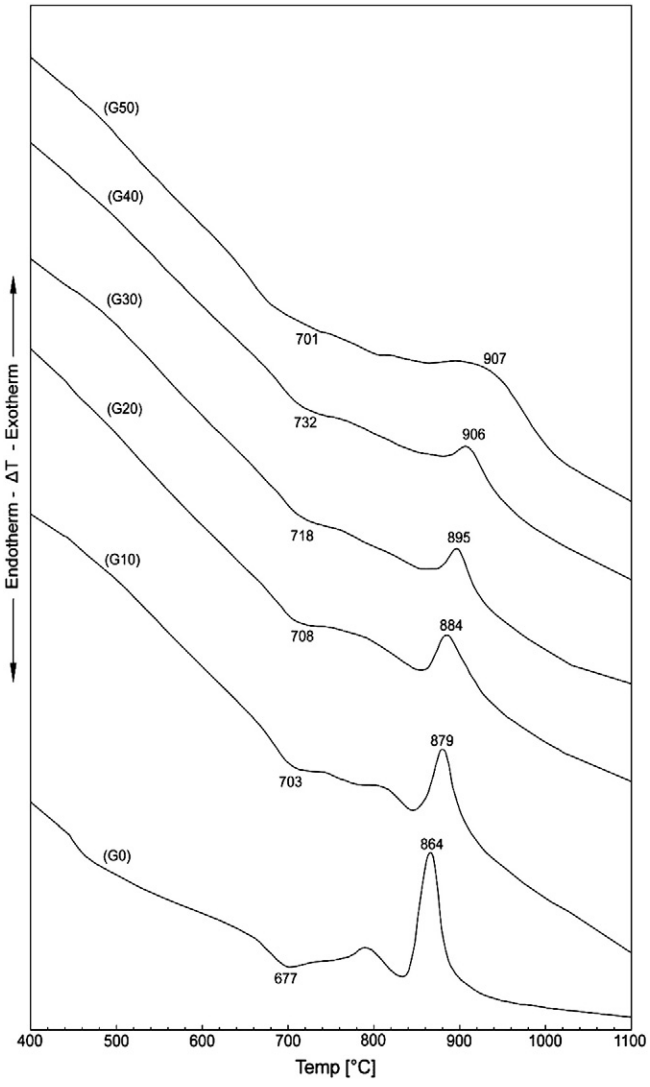

Fig. 1. DTA curves studied of the studied glasses.

Table 3
Thermal behavior of the studied glasses.

Glass no.	Peak temperature (°C)	Thermal effect	Structural changes
G0	665	Minor shallow dip	T_g
	677	Little explicit endothermic peak	Precrystallization process
	864	Sharp exothermic peaks	Crystallization ofaugite + magnetite + anorthite (minor) + olivine (minor)
G10	675	Minor shallow dip	T_g
	703	Little explicit endothermic peak	Precrystallization process
	879	Sharp exothermic peaks	Crystallization of augite + magnetite + anorthite (minor) + olivine (minor)
G20	683	Minor shallow dip	T_g
	708	Little explicit endothermic peak	Precrystallization process
	884	Sharp exothermic peaks	Crystallization of augite + magnetite + anorthite (minor) + olivine (minor)
G30	689	Minor shallow dip	T_g
	718	Little explicit endothermic peak	Precrystallization process
	895	Moderate exothermic peaks	Crystallization of augite + magnetite + anorthite (minor) + olivine (minor) + quartz
G40	702	Minor shallow dip	T_g
	732	Little explicit endothermic peak	Precrystallization process
	906	Broad exothermic peaks	Crystallization of augite + magnetite + anorthite (minor) + olivine (minor) + quartz
G50	680	Minor shallow dip	T_g
	701	Little explicit endothermic peak	Precrystallization process
	907	Broad exothermic peaks	Crystallization of augite + magnetite + anorthite (minor) + olivine (minor) + quartz

X-ray diffraction (Table 3 and Fig. 2) showed that augite, anorthite, magnetite, olivine and quartz were the main crystalline phases developed after heat treatment of the glass samples at 900 °C for 3 h. The occurrence of these phases depends on the base glass composition. In samples G0–G20 augite Ca (Fe, Mg)Si_2O_6, anorthite ($CaAl_2Si_2O_8$), magnetite (Fe_3O_4), olivine (Fe, Mg)$_2SiO_4$ phases were crystallized. In samples G30–G50 the augite seems to be more developed, especially in sample G50 as shown by the increase in the augite lines (e.g. at d-spacing of 2.99, 2.94, 2.91 and 2.54 Å). X-ray examination of glasses heat treated at 900 °C for 3 h revealed that the amounts of augite crystallized in these glasses were greater than nominal amounts. Augite pyroxene seems to represent the major crystalline phase in the fully crystallized specimens. Quartz appears in minor amounts in samples G30 to G50 (e.g. lines 4.24, 3.34 and 1.87 Å). The high frequency of augite phase together with slight observed a little shift of diffraction lines towards higher 2θ values relative to the standard ASTM d-spacing (ASTM powder file 24–203) indicate a significant solid solution most probably of Ca-Tschermak's component $CaAl_2SiO_6$ in augite pyroxene.

After treatment at a higher temperature 1100 °C for 3 h (Fig. 3) the picture of the X-ray patterns became more explicit and nearly approaching the nominal phase constitution. From Figs. 2 and 3 it can be noticed that there are increases in the intensities and explicitly of anorthite lines (e.g. 4.05, 3.78 and 3.18 Å). These phenomena are accompanied by a decrease in intensities of augite lines (e.g. 2.99,

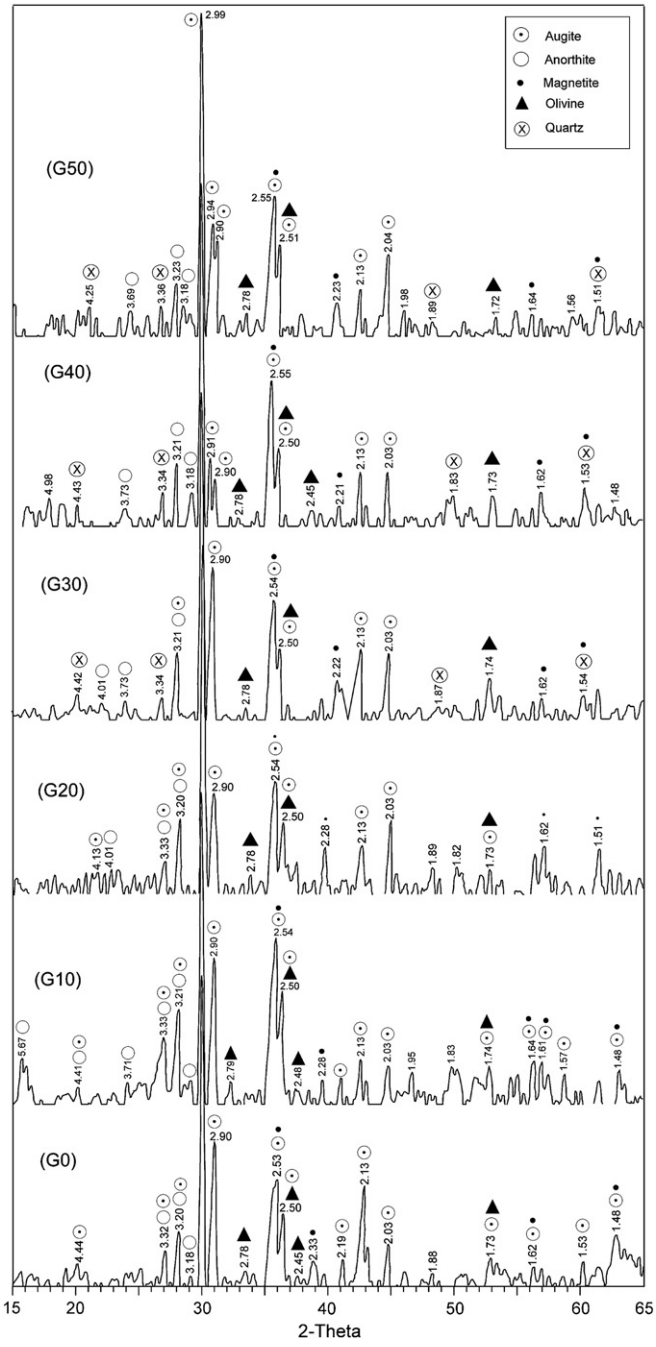

Fig. 2. X-ray diffraction patterns of the studied glasses heat- treated at 900 °C for 3 h.

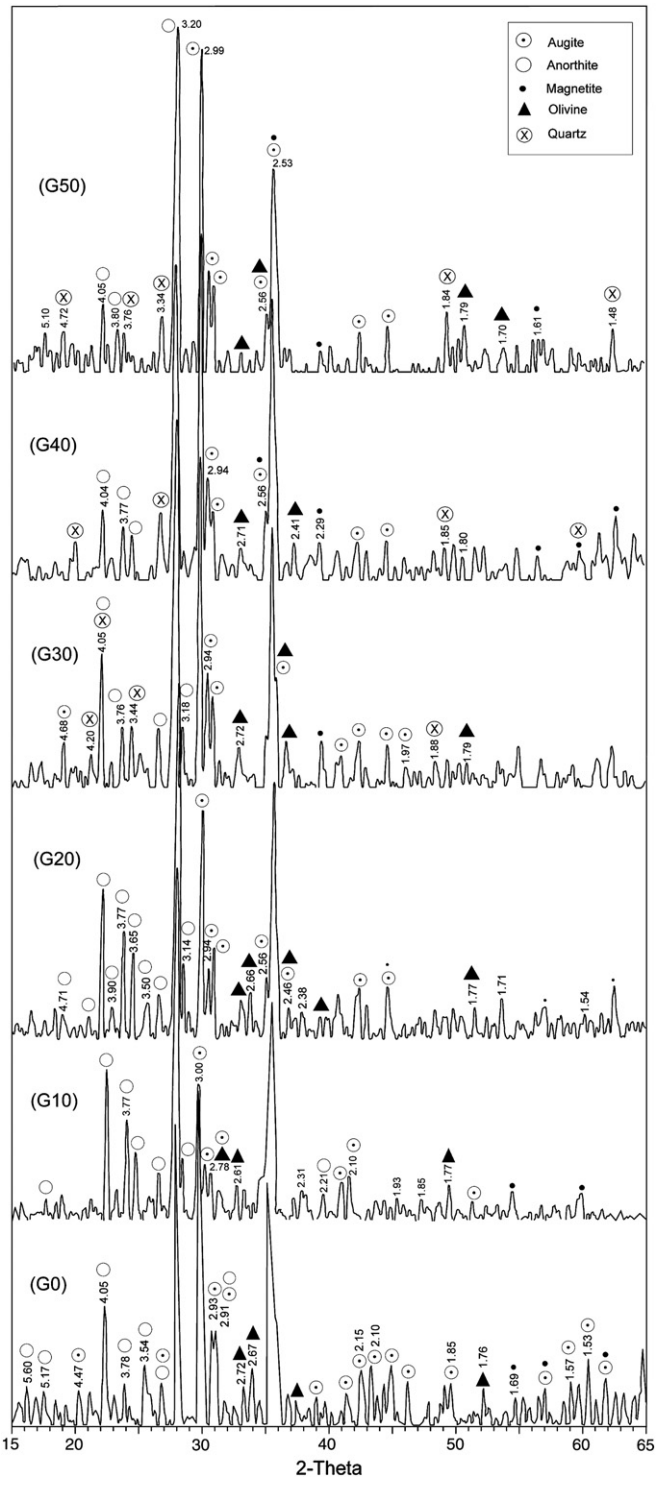

Fig. 3. X-ray diffraction patterns of the studied glasses heat-treated at 1100 °C for 3 h.

Table 4
Crystalline phases developed in the glasses at selected heat-treatment temperatures.

Glass no.	Heat-treatment parameters (°C, h)	Phases developed
G0	900 °C, 3 h	Augite + magnetite + anorthite (minor) + olivine (minor)
	1100 °C, 3 h	Augite + anorthite + olivine + magnetite
G10	900 °C, 3 h	Augite + anorthite (minor) + magnetite + olivine (minor)
	1100 °C, 3 h	Augite + anorthite (minor) + olivine + magnetite
G20	900 °C, 3 h	Augite + magnetite + anorthite (minor) + olivine (minor)
	1100 °C, 3 h	Anorthite + augite + olivine + magnetite
G30	900 °C, 3 h	Augite + anorthite (minor) + magnetite + quartz + olivine (minor)
	1100 °C, 3 h	Augite + anorthite + magnetite + olivine
G40	900 °C, 3 h	Augite + anorthite (minor) + magnetite + quartz + olivine (minor)
	1100 °C, 3 h	Augite + anorthite + magnetite + olivine
G50	900 °C, 3 h	Augite + anorthite + magnetite + quartz + olivine (minor)
	1100 °C, 3 h	Augite + Anorthite + Magnetite + Olivine + Quartz

2.95 and 2.90 Å) particularly in heat treated samples up to 1100 °C for 3 h. It can be said that heat treatment at 1100 °C for 3 h leads to crystallization of augite, anorthite, olivine and magnetite with increasing amounts of anorthite at the expense of augite.

The above mentioned ASTM card 24–203, which had the most precise fitting to the diffractograms of (Figs. 2, 3).

Table 4 gives a summary of the crystalline phases developed after various heat treatment conditions as identified by XRD. The above results emphasize the capability of the expanding pyroxene structure to accommodate different amounts of other cations forming complex series of solid solutions. Thus instead of the formation of the plagioclase molecules $CaAl_2Si_2O_8$, the Ca-Tschermak's component $CaAl_2SiO_6$ are formed which can be accommodated in solid solution in the pyroxene structure.

Figs. 4–9 show photo micrographs of the crystallized specimens. From microscopic examinations of glasses (G0–G50) heat-treated at 1100 °C it can be seen that crystallization began in glasses G0 to G20 by surface nucleation at relatively lower temperatures. While in ceramic waste rich glasses G40–G50 crystallization by both surface and bulk nucleation starts at higher temperatures. The bulk nucleations predominate in G30 to G50, where crystallization readily took place throughout the entire volume of these glasses. The crystal sizes are slightly smaller (Figs. 4–9).

The various properties of the resultant glass-ceramics are listed in (Table 5). The bending strengths of the present glass-ceramics lie in the range 78 to 130 MPa were carried out in glass ceramic samples G0–G50 after treated at 1100 for 3 h. The strengths were increased from G0 to G40 the difference in strength may be attributed to the different major crystalline phases. It is, therefore, found that augite is a more preferable crystalline phase than anorthite from the viewpoint of the strength of these glass-ceramics. A similar tendency was also reported by Park et al. [26] in glass-ceramics prepared from sewage sludge fly ash. They prepared two glass-ceramics with diopside > anorthite and anorthite > diopside, and found that the bending strength of the former glass-ceramic (92 MPa) was higher than that of the latter (75 MPa).

Indentation microhardness measured for the obtained glass-ceramic materials was found to lie in the range 9624 to 10074 MPa which was carried out on glass-ceramic samples G0–G40 treated at 1100 for 3 h. The Vicker's hardness values increased as the content of ceramic waste increased. This indicates the high abrasion resistance of these materials which makes them suitable for many applications under aggressive mechanical conditions.

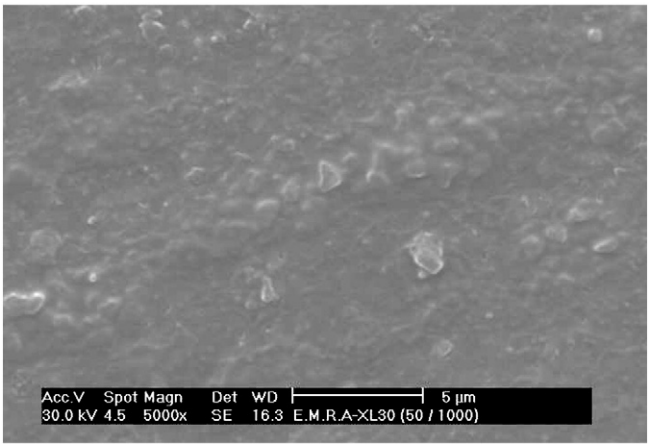

Fig. 5. SEM micrograph of G10 heat- treated at 720 °C for 1 h and then at 1100 °C for 3 h.

5. Discussion

The DTA curves show small dips in the temperature ranging between 665 and 700 °C due to the transition temperature of the glass Tg, or corresponding approximately, in accordance with Devekey and Majumdar [27], to the temperature range defined by Tg and Ts. An increase in the DTA-Tg could be observed as the nominal content

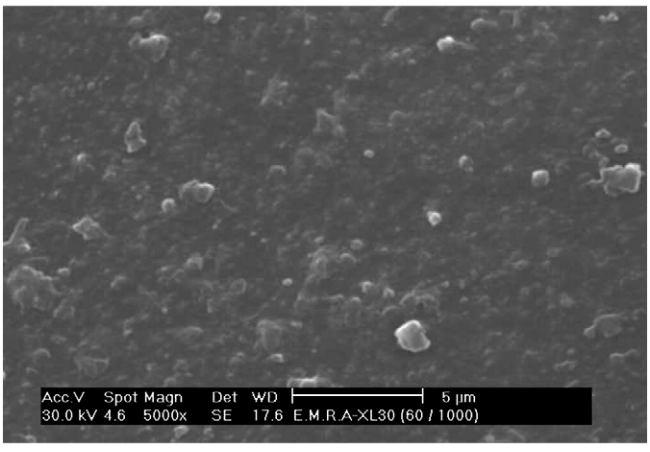

Fig. 4. SEM micrograph of G0 heat-treated at 720 °C for 1 h and then at 1100 °C for 3 h.

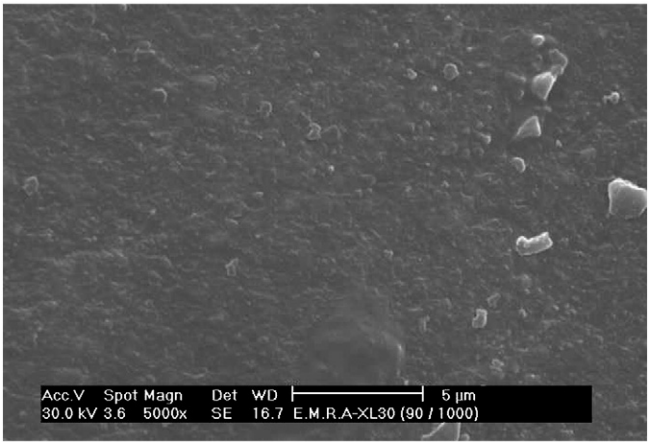

Fig. 6. SEM micrograph of G20 heat-treated at 720 °C for 1 h and then at 1100 °C for 3 h.

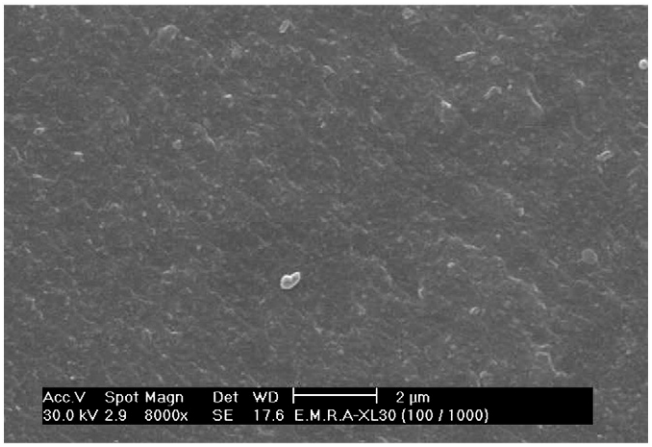

Fig. 7. SEM micrograph of G30 heat- treated at 720 °C for 1 h and then at 1100 °C for 3 h.

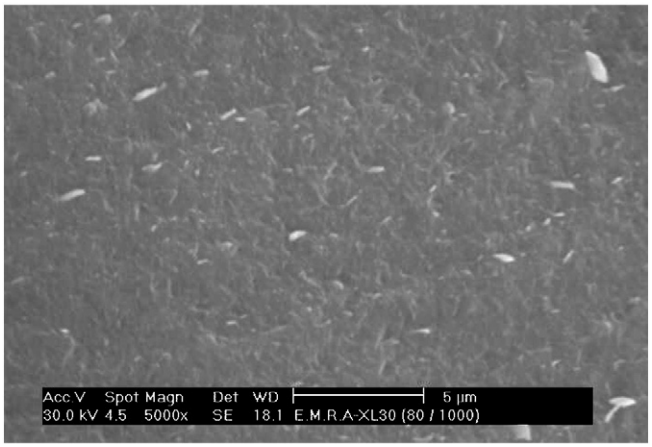

Fig. 9. SEM micrograph of G50 heat-treated at 720 °C for 1 h and then at 1100 °C for 3 h.

of ceramic waste was increased from G0 (665 °C, ceramic waste = 0%) to G40 (700 °C, ceramic waste = 40%).

Another two pertinent features related to the crystallization process could be noticed on the DTA curves. The first feature is the broad endothermic peaks appearing in the temperature range 667–732 °C. These endothermic peaks approximately correspond to phenomenon preceding glass crystallization (pre-crystallization processes), where the glass forming elements begin to arrange themselves in preliminary structural groups suitable for subsequent crystallization [24]. This thermal absorption range will be considered as the nucleation range. The second feature is the major exothermic peaks appearing in the temperature range 864–907 °C immediately following the major endothermic peaks. These exothermic peaks are due to glass devitrification and release of corresponding thermal energy.

XRD results show that the formation about pyroxene phases in quantities are greater than their normative values. This is favored by the tendency of aluminum to share in the building of complex pyroxenes [28].

Augite is the most widespread member of pyroxenes and represents a group of closely related minerals with chemical formula of Ca (Mg, Fe, Al) (Si Al) O_6, identical in structure, but containing different percentages of certain elements [29]. In the light of the experimental results it can be considered that there is an intermediary member between diopside ($CaMgSi_2O_6$) and Ca-Tschermak ($CaAl_2SiO_6$). This member represents a mineral midway between these two minerals along this series, where Al^{3+} occupies both octahedral (AlO_6) and tetrahedral (AlO_4) position in the structure.

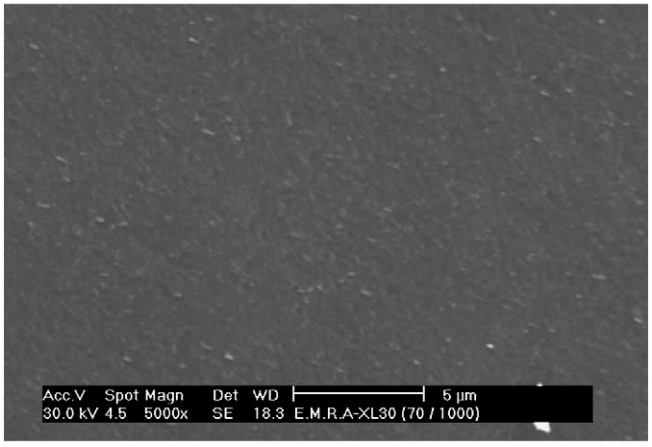

Fig. 8. SEM micrograph of G40 heat- treated at 720 °C for 1 h and then at 1100 °C for 3 h.

Salama et al. [23] determined the maximum concentrations of the of $CaAl_2SiO_6$ component, which can be taken up by diopside as 25%. Omar et al. [30] showed that complex pyroxene containing up 48% of the $CaAl_2SiO_6$ component under non-equilibrium conditions of crystallization could obtained. Ca-Tschermak ($CaAl_2SiO_6$) is a pyroxene phase. The amount of aluminum sharing in the pyroxene structure is dependent upon the original composition of the glass and the crystallization parameters. Flemming and Luth [31] studied the system of $CaMgSi_2O_6$–$CaAl_2SiO_6$. They showed that the composition across the diopside-Ca-Tschermak's solid solution follow the general formula:

$$\underset{\text{Octahedral sublattice}}{Ca\,[Mg1-x,\ Al\ x]}\ \underset{\text{tetrahedral sublattice}}{(Si(1-x)/2,\ Al\ x/2)_2O_6}$$

The displacement of the major characteristics d-spacing lines of the pyroxene variety towards higher 2θ values may support the suggestion that Al^{3+} was incorporated in the pyroxene ss of diopside type. It was previously mentioned by Omar and El-Shennawi [28] that during the crystallization of basaltic and similar basic silicate melts the boundary curves between the plagioclase and pyroxene fields of crystallization is displaced towards widening of the crystallization field of complex aluminous pyroxene phases.

SEM results show that, as the ceramic waste component (or more specifically its Al_2O_3 ingredients) in the glass increases, the tendency of the glass through bulk crystallization increases. At about 30 wt.% ceramic waste (i.e.G30) the tendency towards bulk crystallization increases and it is therefore possible to relate such a high tendency towards bulk crystallization to the effect played by Al^{3+} ions. Al^{3+}

Table 5
Physical tests of the studied glass.

Properties glass no.	Heat-treatment parameters (°C, h)	Hardness (MPa)	Bending strength (MPa)	Phases developed
G0	1100	9624	92	Augite + anorthite + olivine + magnetite
G10	1100	9771	98	Augite + anorthite + olivine + magnetite
G20	1100	9967	110	Augite + anorthite + olivine + magnetite
G30	1100	10,006	123	Augite + anorthite + olivine + magnetite
G40	1100	10,074	135	Augite + anorthite + olivine + magnetite
G50	1100	9947	132	Augite + anorthite + olivine + magnetite

Ions may likewise be responsible for encouraging bulk crystallization on going from G0 to G50 as a result of a possible change in its coordination from four to six. The coordination state of Al^{3+} ions in silicate glasses has been subject to considerable debate. Physical property measurements on alkali silicate glasses [32] and alkaline earth silicate melts [33] suggested that Al_2O_3 acts amphoterically over a wide range of compositions. Aluminum can also occur in both network forming and network modifying positions, and that Al^{3+} ions would therefore in both fourfold and six fold coordination.

The mechanism of surface crystallization in the glasses (G0–G20) may be explained as follows. When a high ferrous iron-containing silicate glass is heat-treated in an oxidizing environment, the cations diffuse from the interior towards the surface. Transition cations, e.g. Fe^{2+}, undergo chemical oxidation during the diffusion of cations toward the surface [34]. The overall mechanism of the diffusion of cations towards the surface in a glass is well described by Cooper et al. [34]. According to them, heat-treatment in an oxidizing atmosphere results in an enrichment of Ca^{2+} and Mg^{2+} at the free surface. The outward diffusion of Ca^{2+} and Mg^{2+} is accompanied by a counter flux of the positively charged electron holes that move toward the interior of the sample and hence cause oxidation of Fe^{2+} to Fe^{3+}.

Generally speaking, as the basaltic rocks content increases in the base composition and consequently ceramic waste decreases, the crystallization is easier (i.e. the glass is more crystallizable) and crystallization began at lower temperatures, and vice versa. This is most probably due to the role played by Na_2O Fe_2O_3 and TiO_2 in basaltic composition, which is acting as nucleating agents in the iron reach glasses, and are known to reduce the viscosity of the melt, and consequently the mobility and diffusion of ions of the corresponding glasses are increased [35].

6. Conclusion

Saudi basalts from Harrat Kishb with ceramic waste materials from Saudi Ceramic Factories can be successfully used for making glass-ceramics materials that have excellent properties. The present results show that the increase of ceramic waste material in glass results, in increased bulk crystallization. This effect is accompanied by a change in the texture of the glass-ceramic specimens from coarse to fine grained augite, anorthite, olivine, magnetite which were formed during heat-treatment. The final samples are characterized by, zero water absorption and low-cost manufacture cycle; the mechanical characteristics significantly surpass these of the traditional ceramics. The microstructure, bending strength and microhardness results showed that the best among the glasses tested was G40, with the composition of 60% basaltic rocks and 40% ceramic waste. These glass-ceramics can be used for different purposes such as floor and wall tiles, and many other products.

References

[1] P.W. McMillan, Glass-ceramics, 2nd ed Academic Press, London, 1979.
[2] S.Yilmaz, The investigation of production conditions and properties of basalt glass ceramics from the volcanic basalt rocks. Ph.D. thesis, Istanbul Technical University, Istanbul, 1977.
[3] M. Erol, S. Kucukbayrak, Ae Mercboyu, M.L. Ovecoglu, Crystallization behavior of glasses produced from fly ash, J. Euro Ceram. Soc. 21 (2001) 2835–2841.
[4] S.N. Salama, S.M. Salman, H. Darwish, The effect of nucleating catalysts on crystallization characteristics of aluminosilicate glasses, Ceram. Silik. 46 (1) (2002) 15–23.
[5] A. Karamanov, M. Pelino, Crystallization phenomena in iron-rich glasses, J. Non-Cryst. Solids 28 (1–3) (2001) 139–151.
[6] A.W.A. El-Shennawi, M.A. Mandour, M.M. Morsi, S.A. Abdel-Hameed, Monopyroxenic basalt-based glass-ceramics, J. Am. Ceram. Soc. 82 (50) (1999) 1181–1186.
[7] Senol Yilmaz, Gunhan Bayrak, Saduman Sen, Ugur Sen, Structural characterization of basalt-based glass-ceramic coating, Mater. Des. 27 (2006) 1092–1096.
[8] Alexander Karamanov, Sibel Ergul, Mustafa Akyildiz, Mario Pelino, Sinter-crystallization of a glass obtained from basaltic tuffs, J. Non-Cryst. Solids 354 (2008) 290–295.
[9] Alexander Karamanov, Lorenzo Arrizza, Sibel Ergul, Sintered material from alkaline basaltic tuffs, J. Eur. Ceram. Soc. 29 (2009) 595–601.
[10] G.A. Khater, Diopside-anorthite-wollastonite glass-ceramics based on waste from granite quarries, Glass Technol.: Eur. J. Glass Sci. Technol. A 51 (1) (2010) 6–12.
[11] G.A. Khater, Glass-ceramics in the CaO-MgO-Al_2O_3-SiO_2 system based on industrial waste materials, J. Non-Cryst. Solids 356 (2010) 3066–3070.
[12] G.A. Khater, E.M. Hamzawy, Glass- ceramic based on Saudi Arabia basalt and glass cullet wastes, Ceramurgi and Ceram. Acta 1 (2010) 15–19.
[13] G.A. Khater, M.M. Morsi, Glass-ceramics based on spodumene-enstatite system from natural raw materials, Thermochim. Acta 519 (2011) 6–11.
[14] D.F. Bickford, C.M. Jantzen, Devitrification of defense nuclear waste glass: role of melt insoluble, J. Non-Cryst. Solids 84 (1986) 299–307.
[15] I.W. Donald, B.L. Metcalfe, R.N. Taylor, Review-the immobilization of high level radioactive waste using ceramics and glasses, J. Mater. Sci. 32 (1997) 5851–5887.
[16] M.I. Ojovan, W.E. Lee, New development in glassy nuclear waste forms, Nova Scientific Publisher, New York, 2007.
[17] A. Karamanov, P. Pisciella, C. Cantalini, M. Pelino, Influence of the Fe^{3+}/Fe^{2+} ratio on the crystallization of iron-rich glasses made with industrial wastes, J. Am. Ceram. Soc. 81 (2000) 3153–3157.
[18] P. Kavouras, P. Komninou, K. Chrissafis, Microstructural changes of processed vitrified solid waste products, J. Eur. Ceram. Soc. 23 (2003) 1305–1311.
[19] A.A. Francis, R.D. Rawlings, R. Sweeney, Crystallization kinetic of glass particles prepared from a mixture of coal ash and soda-lime cullet glass, J. Non-Cryst. Solids 333 (2004) 187–193.
[20] A. Karamanov, M. Aloisi, M. Pelino, Vitrification of copper flotation waste, J. Hazard. Mater. 140 (2007) 333–339.
[21] P. Kavouras, T. Kehagias, I. Tsilika, G. Kaimakamis, K. Chrissafis, S. Kokkou, D. Papadopoulos, Th. Karakostas, Glass-ceramic materials from electric arc furnace dust, J. Hazard. Mater. A139 (2007) 424–429.
[22] S.A.M. Abdel-Hameed, I.M. Bakr, Effect of alumina on ceramic properties of cordierite glass-ceramic from basalt rock, J. Eur. Ceram. Soc. 27 (2007) 1893–1897.
[23] S.N. Salama, H. Darwish, H.A. Abo-Mosallam, Crystallization and properties of glasses based on diopside-Ca-Tschermak's-fluorapatite system, J. Eur. Ceram. Soc. 25 (2005) 1133–1142.
[24] A.W.A. El-Shennawi, The use of differential thermal analysis in the study of glass-ceramics, Ain Shams Sci. Bull. 24 (1983) 225–244.
[25] R.L. Thakur, S. Thiagarajan, Studies in catalyzed crystallization of glasses, Inst. Bull. 13 (2) (1966) 33.
[26] Y.J. Park, S.O. Moon, J. Heo, Crystallization phase control of glass ceramics obtained from sewage sludge fly ash, Ceram. Int. 29 (2003) 223–227.
[27] R.C. Devekey, A.J. Majumdar, Nucleation and crystallization studies of some glasses in the CaO-MgO-Al_2O_3-SiO_2 system, Miner. Mag 37 (1970) 771.
[28] A.A. Omar, A.W.A. El-Shennawi, Crystallization of some molten Egyptian basaltic rocks and corresponding glass. U.A.R. J. Geol. 15 (1) (1971) 65–73.
[29] N.M. Pavlushkin, Principals of Glass Ceramics Technology, 2nd ed. Stroiizdat, Moscow, 1979 (in Russian).
[30] A.A. Omar, S.M. Salman, M.Y. Mahmoud, Phase relations in the diopside-anorthite-akermanite system, Ceram. Int. 12 (1986) 53–59.
[31] L.R. Flemming, R.W. Luth, Si MAS NMR study of diopside-Ca-Tschermak clinopyroxenes: detecting both tetrahedral and octahedral Al substitution, Am. Mineral. 87 (2002) 25–36.
[32] R.M. Douglas, The crystal Structure of anorthite, Am.Mineral. 43 (5–6) (1958) 517.
[33] R.H. Rein, J. Chipman, Activities in the liquid solution SiO_2-CaO-MgO-Al_2O_3 at 1600°C, Trans. AIME 233 (2) (1965) 415–425.
[34] R.D. Cooper, J.B. Fanselow, D.B. Pocker, The mechanism of oxidation of a basaltic glass: chemical diffusion of network-modifying cations, Geochimica et Cosmochimica Acta 60 (1996) 3253–3265.
[35] G.H. Beall, H.L. Rittler, Basalt glass-ceramics, Am. Ceram. Bull. 55 (1976) 579–582.